Discovery and characterization of [(cyclopentyl)ethyl]benzoic acid inhibitors of microsomal prostaglandin E synthase-1

Katherine M. Partridge, Stephen Antonysamy, Shobha N. Bhattachar, Srinivasan Chandrasekhar, Matthew J. Fisher, Adrian Fretland, Karen Gooding, Anita Harvey, Norman E. Hughes, Steven L. Kuklish, John G. Luz, Peter R. Manninen, James E. McGee, Daniel R. Mudra, Antonio Navarro, Bryan H. Norman, Steven J. Quimby, Matthew A. Schiffler, Ashley V. Sloan, Alan M. Warshawsky, Jennifer M. Weller, Jeremy S. York, Xiao-Peng Yu

PII: S0960-894X(16)31151-9
DOI: http://dx.doi.org/10.1016/j.bmcl.2016.11.011
Reference: BMCL 24406

To appear in: *Bioorganic & Medicinal Chemistry Letters*

Received Date: 9 September 2016
Revised Date: 3 November 2016
Accepted Date: 4 November 2016

Please cite this article as: Partridge, K.M., Antonysamy, S., Bhattachar, S.N., Chandrasekhar, S., Fisher, M.J., Fretland, A., Gooding, K., Harvey, A., Hughes, N.E., Kuklish, S.L., Luz, J.G., Manninen, P.R., McGee, J.E., Mudra, D.R., Navarro, A., Norman, B.H., Quimby, S.J., Schiffler, M.A., Sloan, A.V., Warshawsky, A.M., Weller, J.M., York, J.S., Yu, X-P., Discovery and characterization of [(cyclopentyl)ethyl]benzoic acid inhibitors of microsomal prostaglandin E synthase-1, *Bioorganic & Medicinal Chemistry Letters* (2016), doi: http://dx.doi.org/10.1016/j.bmcl.2016.11.011

Discovery and characterization of [(cyclopentyl)ethyl]benzoic acid inhibitors of microsomal prostaglandin E synthase-1

Katherine M. Partridge,[a,*] Stephen Antonysamy,[b] Shobha N. Bhattachar,[a] Srinivasan Chandrasekhar,[a,c] Matthew J. Fisher,[a] Adrian Fretland,[a,d] Karen Gooding,[a,c] Anita Harvey,[a,c] Norman E. Hughes,[a] Steven L. Kuklish,[a] John G. Luz,[b] Peter R. Manninen,[a] James E. McGee,[a] Daniel R. Mudra,[a] Antonio Navarro,[a] Bryan H. Norman,[a] Steven J. Quimby,[a] Matthew A. Schiffler,[a] Ashley V. Sloan,[a] Alan M. Warshawsky,[a] Jennifer M. Weller,[a] Jeremy S. York,[a] Xiao-Peng Yu,[a]

[a]Lilly Research Laboratories, A Division of Eli Lilly and Company, Indianapolis, Indiana 46285, USA

[b]Eli Lilly Biotechnology Center, San Diego, CA 92121, USA

Present/Permanent address:

[c]Retired

[d]Discovery Sciences, Oncology Innovative Medicines Unit, AstraZeneca R&D Boston, 35 Gatehouse Drive, Waltham, MA 02451, USA

Abstract

We describe a novel class of acidic mPGES-1 inhibitors with nanomolar enzymatic and human whole blood (HWB) potency. Rational design in conjunction with structure-based design led initially to the identification of anthranilic acid **5**, an mPGES-1 inhibitor with micromolar HWB potency. Structural modifications of **5** improved HWB potency by over 1000×, reduced CYP2C9 single point inhibition, and improved rat clearance, which led to the selection of [(cyclopentyl)ethyl]benzoic acid compound **16** for clinical studies. Compound **16** showed an

IC_{80} of 24 nM for inhibition of PGE_2 formation *in vitro* in LPS-stimulated HWB. A single oral dose resulted in plasma concentrations of **16** that exceeded its HWB IC_{80} in both rat (5 mg/kg) and dog (3 mg/kg) for over twelve hours.

Graphical Abstract

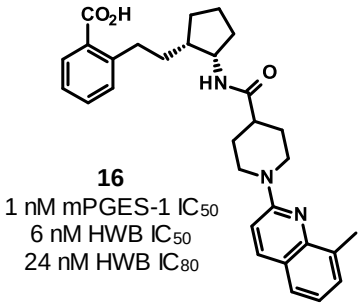

16
1 nM mPGES-1 IC_{50}
6 nM HWB IC_{50}
24 nM HWB IC_{80}

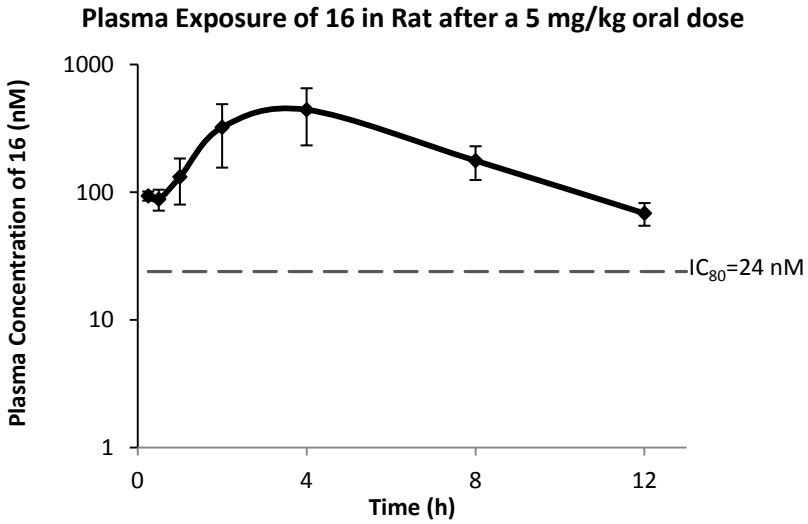

Corresponding Author:

* (K.M.P.) E-Mail: Partridge_Katherine@lilly.com Tel: +1-317-433-0465.

Keywords: mPGES-1**,** Prostaglandin pathway**,** bioavailability**,** Biomarker

Arthritic pain is a leading cause of disability in the United States.[1] Common treatments for the initial stages of arthritis rely heavily on NSAIDs (non-steroidal anti-inflammatory drugs) and

cyclooxygenase-2 (COX-2) inhibitors to provide analgesia.[2] Both classes of pharmaceuticals block the cyclooxygenase (COX)-catalyzed conversion of arachidonic acid (AA) to prostaglandin H_2 (PGH_2), which is rapidly converted to an array of bioactive prostanoids; including TXA_2, PGE_2, PGD_2, PGI_2, and $PGF_{2\alpha}$ (Figure 1). Prostaglandin E_2 (PGE_2) is thought to be the main mediator of pain and inflammation, and the resulting downstream suppression of PGE_2 gives NSAIDs and COX-2 inhibitors their analgesic properties.[3]

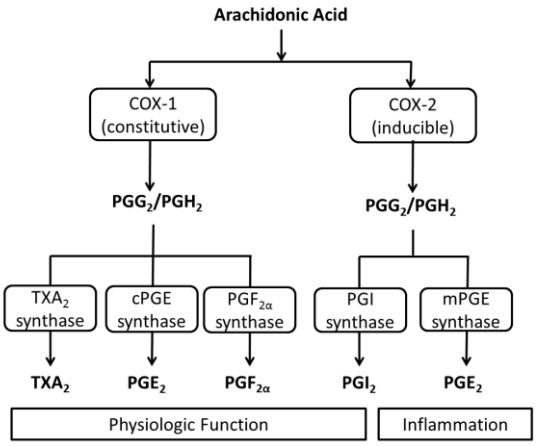

Figure 1. Primary biosynthetic pathways of select prostanoids

NSAIDs non-selectively inhibit two isoforms of cyclooxygenase, COX-1 and COX-2. COX-1 is constitutively expressed in most tissues and is important for regulating homeostatic physiologic tasks, including gastric cytoprotection and kidney function.[4] COX-2 expression is inducible and upregulated under inflammatory conditions, allowing increased production of prostaglandins.[5] The coincidental COX-1 inhibition found with traditional NSAIDs is thought to give rise to the increased risk of gastric bleeding and ulcerations found with this class of analgesics.[6] COX-2 selective inhibitors were developed as a means to target inflammatory pain while providing the potential for reduced risk of GI complications.[7] Selective COX-2 inhibitors are efficacious and appear to have a more tolerable GI profile than NSAIDs, however they have been found to carry an increased cardiovascular risk, which is thought to arise from COX-2 derived suppression of PGI_2.[8] A more selective inhibitor of inducible PGE_2 formation is an attractive strategy for mediation of nociception with a lower risk of the side effects that result from the indiscriminate suppression of other prostanoids.[9]

Of the prostaglandin E synthases (PGES) known to convert PGH_2 to PGE_2, only microsomal PGES-1 (mPGES-1) expression is upregulated under inflammatory conditions.[10] Additionally, the expression of mPGES-1 and COX-2 has been shown to be coupled.[11] Evidence for the key role of mPGES-1 in inflammatory pain comes from murine knockouts, which demonstrated reduced response in inflammatory pain models and resistance towards disease development in collagen-induced arthritis models.[12] These observations suggest that a selective inhibitor of mPGES-1 may offer the analgesic properties of traditional NSAIDs with a reduced side effect profile. Work in this area has produced a wide range of chemotypes, including compounds with both neutral and acidic moieties, for example **1**–**4** (Figure 2).[13]

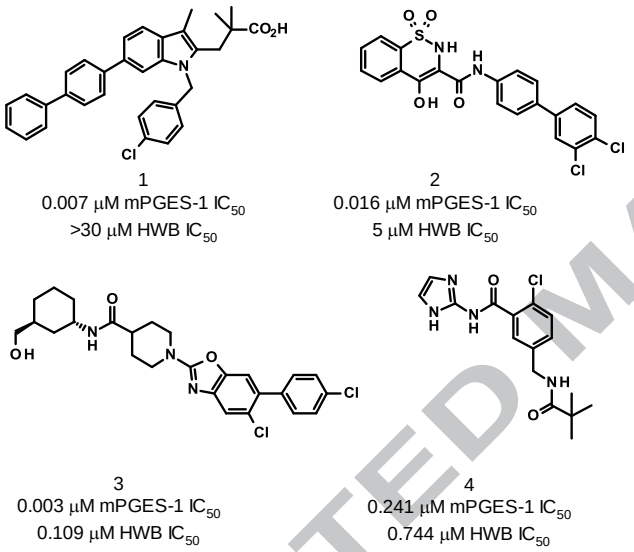

Figure 2. Representative mPGES-1 Inhibitors

To support the discovery of new molecules, enzymatic and native tissues assays have been developed to assess the potency of mPGES-1 inhibitors. A cell-free assay using a microsomal preparation assay of human mPGES-1 from HEK-293 cells was used to provide a direct measure of enzyme inhibition.[14] It is also known that mPGES-1 inhibitors impede the formation of PGE_2 in *in vitro* LPS-stimulated human whole blood (HWB).[13a] Historically, this assay has been a critical component of both NSAID and COX-2 inhibitor development. Pasqua has shown that the inhibition of PGE_2 production in HWB at the IC_{80} level for a variety of NSAIDs and COX-2 analgesics correlated with plasma drug concentrations of the clinically efficatious dose.[15] The reduction of PGE_2 in HWB provides a seamless biomarker linking *in vitro* preclinical and the *in vivo* clinical observations.[16]

The high-resolution X-ray crystal structure of mPGES-1, a homotrimeric protein, has recently been published and has facilitated the development of new inhibitors through rational design.[17] In our laboratories, this led to the discovery and development of compound **4** (Figure 2). Building on our understanding of the mPGES-1 binding site, we used structure-based drug design to create a new class of mPGES-1 inhibitors. In this manuscript, we describe the discovery and characterization of a series of potent, orally bioavailable cyclopentylethylbenzoic acid inhibitors of mPGES-1.

In the X-ray co-crystal of mPGES-1 and compound **4** (Figure 3),[13e] the central hydrophobic core of **4** rests directly above the sulfur of the glutathione cofactor, and its substituents project down the left and right shallow flanking grooves. This binding mode takes advantage of the dense arrangement of hydrogen bond donors surrounding the opening to the glutathione binding pocket. In addition to a direct hydrogen bond with His53, compound **4** interacts with both Arg52 and Thr131 through ordered water molecules. We hypothesized that a similarly shaped molecule, with a properly oriented carboxylic acid, could form a direct salt bridge with Arg52, effectively replacing the imidazole. In order to retain the orientation of the *tert*-butyl amide in the right hand groove, we adjusted the central constraint by replacing the aromatic core with a five-membered aliphatic moiety. We designed and synthesized compound **5**, which was found to inhibit mPGES-1 with an IC_{50} of 43 nM and a HWB IC_{50} of 8.9 μM. The X-ray co-crystal structure of **5** and mPGES-1 showed that the inhibitor adopts a similar binding mode to **4**, maintaining the five membered hydrophobic ring over the glutathione, as predicted. The central ring allowed the critical pivaloyl amide moiety to correctly project into the right hand groove. As designed, the carboxylate of compound **5** formed a hydrogen bond with His53 and also made a direct hydrogen bond to Arg52 and a van der Waals contact with Thr131.

a.

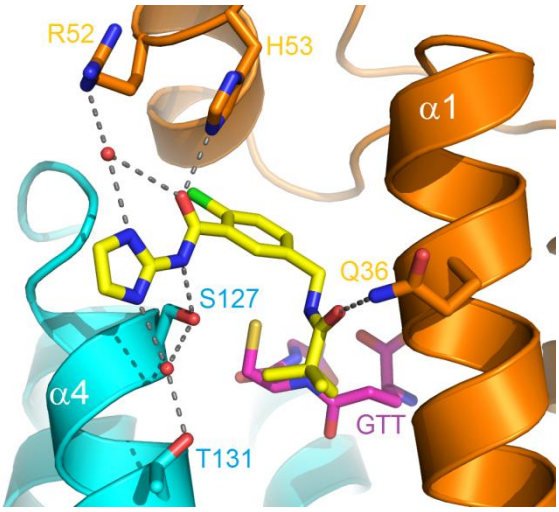

b.

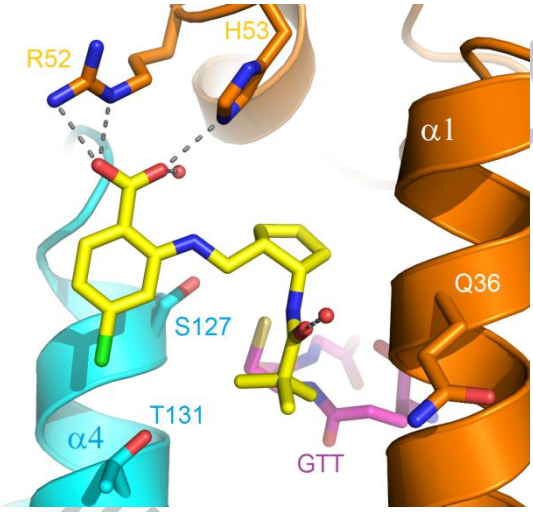

Figure 3. X-ray co-crystal structure of mPGES-1 with **4** and *rac*-**5**

A. mPGES-1 bound to compound 4 (represented as sticks and colored by atom: C, yellow; N, blue; O, red; Cl, green). Glutathione is presented as sticks and colored by atom as above except C is magenta and S is tan. Chain 1 is orange and represented by cartoon. Side chains of chain 1 are represented as sticks and colored as above except C is orange. Chain 2 is cyan and represented by cartoon. Side chains of chain 1 are represented as sticks and colored as above except C is cyan.

B. mPGES-1 bound to rac-5. Representations and color assignments same as in (A)

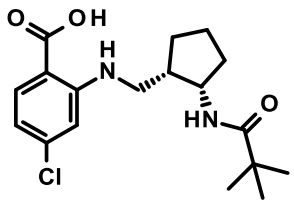

5

0.043 μM mPGES-1 IC_{50}

8.91 μM HWB IC_{50}

While compound **5** displayed good enzymatic inhibitory activity, most of the potency did not translate to the more physiologically relevant whole blood environment. Replacing the pivaloyl amide of compound **5** with larger substituents, such as *N*-aryl piperidines (Table 1, compounds **6** and **7**) improved the potency in enzymatic and HWB assays. Although compounds **6** and **7** had similar IC_{50} values in the enzymatic assay (2 and 4 nM), compound **7** was 30 times more potent in HWB. To support the notion that the suppression of PGE_2 in HWB was due to inhibition of mPGES-1 and not COX-1 or COX-2, compounds **6** and **7** were tested in an A549 cellular assay which tested the production of multiple prostanoids. In this assay, **6** and **7** inhibited the formation of PGE_2 (IC_{50} = 0.021 μM and 0.0035 μM, respectively) but not PGI_2. Additionally, in LPS stimulated HWB, **6** and **7** disrupted neither TXB_2 nor $PGF_{2\alpha}$ production. These data suggest that the observed inhibition of PGE_2 formation in HWB was due to inhibition of mPGES-1and not COX-1 or COX-2. While the IC_{50} was a useful metric early in the SAR studies, the HWB IC_{80} is a more clinically relevant value.[15] Therefore, we chose to benchmark all future potency against the latter standard.

Compound **7** had single-digit nanomolar potency in HWB, but we identified at least two characteristics that needed improvement. First, this compound had moderate clearance in the rat (Cl = 40 mL/(min*kg)). Second, **7** inhibited CYP2C9 in a single-point microsomal preparation assay (71% inhibition at 10 μM). Therefore, further work aimed to identify compounds with HWB activity similar to **7**, while simultaneously reducing both the rat clearance and CYP inhibition liabilities.

We continued our SAR studies by examining the linker between the cyclopentane and the aromatic ring. The oxygen linked salicylic acid **8** demonstrated a modestly increased in HWB IC_{80}, a decreased in CYP2C9 single point inhibition, and a slightly increased rat clearance relative to anthranilic acid **7**. Compound **9**, an alkyl substituted benzoic acid, had similar HWB potency and CYP2C9 single point inhibition to **7**, but had lower clearance. The observed decrease in clearance without an associated attenuation of CYP2C9 single-point inhibition suggested that rat clearance was not driven solely by the apparent CYP2C9 interaction.

The improved clearance of compound **9** focused our attention on other 2-alkylbenzoic acid derivatives. Replacement of the chloro- substituent of compound **9** yielded analogs **10–12**, which had similarly low rat clearance. Toluic acid **10** was 2× less potent in HWB than analog **9**, while fluoro- and hydrogen substitutions (**11**-**12**) resulted in approximately an order of magnitude loss in potency. Unsubstituted benzoic acid **12** showed minimal inhibition of CYP2C9. Within the confines of the single point changes between compounds **9–12**, decreased CYP2C9 inhibition appeared to correlate with decreased lipophilicity as characterized by the calcuclated logD at pH 7.4. Nicotinic acid **13** was 4× less potent than parent benzoic acid **12** and had higher clearance in the rat.

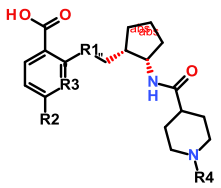

Table 1. SAR of mPGES-1 Inhibitors **6–16**

Cmpd	R_1	R_2	R_3	R_4	cLogD, 7.4[a]	mPGES-1 IC_{50} (nM)[b]	HWB PGE2 IC_{50} (nM)[b]	HWB IC_{80} (nM)[b]	Rat Clearance, IV (mL/(min*kg))[c]	% inhibition of CYP2C9 @ 10 µM
6[d]	NH	Cl	CH	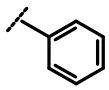	2.07	2	81	1371	81 (34)	46
7	NH	Cl	CH	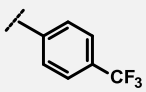	2.95	4	3	8	40 (14)	71

8	O	Cl	CH	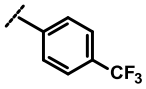	2.08	2	8	25	57 (22)	39
9	CH_2	Cl	CH	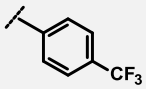	3.25	1	1	5	16 (11)	51
10	CH_2	Me	CH	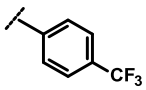	3.27	1	3	10	9 (3)	56
11	CH_2	F	CH	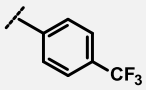	2.88	1	6	41	12 (2)	40
12	CH_2	H	CH	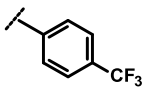	2.65	2	5	40	5 (0.6)	5
13	CH_2	H	N	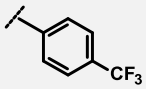	1.44	6	21	146	38 (1)	ND
14	CH_2	H	CH	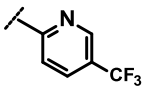	2.11	2	34	267	6(3)	22
15	CH_2	H	CH	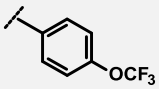	3.24	1	10	43	17(5)	32
16	CH_2	H	CH	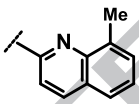	3.15	1	6	24	31 (4)	14

[a] Values are reported as geometric means of a minimum of three samples [b] Calculated using Marvin and calculator plugin freeware (www.chemaxon.com, ChemAxon Kft, Budapest, Hungary) [c] a 1 mg/kg IV dose. Data is a mean of three animals, standard deviation in parentheses. Pharmacokinetic calculations were performed using Watson Version 7.4 [d] Compound is a racemic mixture; all other compounds are single enantiomers

Because of the HWB potency, low clearance, and low CYP2C9 single point inhibition associated with compound **12**, the cyclopentylethyl benzoic acid core was held constant while other *N*-aryl piperidine carboxamides were examined (compounds **14**–**16**). These analogs had similar apparent CYP2C9 single point inhibition and rat clearance but exhibited different potencies. Replacing the trifluoromethyl substituent of **12** with a trifluoromethoxy group had a negligible impact on potency. The 5-trifluoropyridyl analog **14** was less potent than **12** in HWB, and 8-methylquinoline analogue **16** was slightly more potent. With high *in vitro* potency, low

CYP2C9 inhibition, moderate rat clearance, compound **16** was selected for further characterization.

The X-ray co-crystal of **16** with mPGES-1 shows that the benzoic acid of **16** forms a bidentate salt bridge to Arg52 and coordinates to His53 through a water bridge. The central hydrophobic cyclopentane ring rests above glutathione, projecting the amide substituent down the hydrophobic groove. The N-aryl piperidine rests in the hydrophobic cleft with interactions dominated by van der Waals contacts with Tyr28, Ile32, Tyr130, and Gln134. The methyl substituent of the quinoline projects deeply into a cleft behind Ile32.[18]

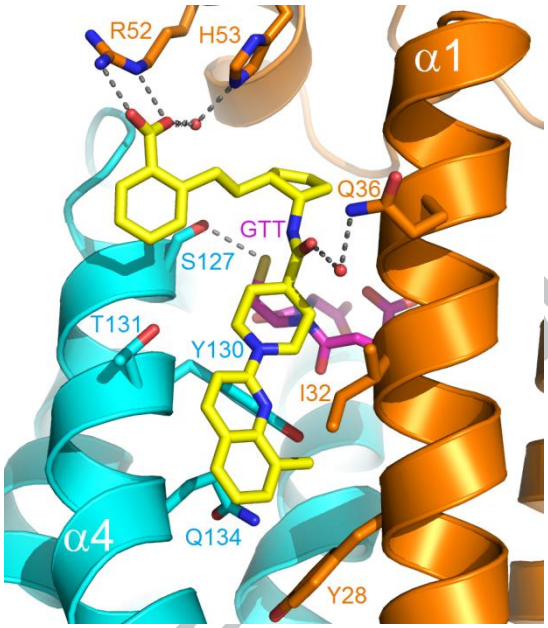

Figure 4. X-ray co-crystal structure of mPGES-1 with **16**

mPGES-1 bound to compound 16 (represented as sticks and colored by atom: C, yellow; N, blue; O, red; Cl, green). Glutathione is presented as sticks and colored by atom as above except C is magenta and S is tan. Chain 1 is orange and represented by cartoon. Side chains of chain 1 are represented as sticks and colored as above except C is orange. Chain 2 is cyan and represented by cartoon. Side chains of chain 1 are represented as sticks and colored as above except C is cyan.

In contrast to celecoxib, compound **16** suppressed neither PGI_2 formation in the A549 assay nor TXB_2 or $PGF_{2\alpha}$ production in HWB at concentrations up to 10 μM. Furthermore, no inhibition of either COX-1 or COX-2 was observed with 10 μM, thus **16** is at least 10,000-fold

selective against those enzymes. Upon testing against a DiscoverX panel of 35 receptors and ion channels, **16** did not display any activity that we deemed to present an undue risk. No activity was detected against hERG at 10 μM **16** in a CEREP assay. Taken together, these biochemical data supported the characterization of **16** as a selective inhibitor of mPGES-1.

The pharmacokinetic profiles of **16** were determined in both rat and dog. The volume of distribution at steady state was 4.8 L in the rat and 1.2 L in the dog. Clearances of less than hepatic blood flow were observed in both species at an IV administered dose of 1 mg/kg. The oral bioavailability exceeded 50% in both species.

Table 2. Pharmacokinetic Properties of **16**[a]

Species	Dose IV/Oral (mg)	Clearance, IV (mL/min/kg)	Volume of Distribution at Steady State, IV (L/kg)	Maximum oral concentration (μM)	Oral Bioavailability (%)
Rat	1/5	31 (4)	4.8(1.8)	0.53 (0.14)	52 (12)
Dog	1/3	6.5 (1.7)	1.2(0.6)	4.0 (1.3)	68 (26)

[a] Data is a mean of three animals. Standard deviation reported in parentheses. Pharmacokinetic calculations were performed using Watson Version 7.4

As shown in Figure 5, with a 5 mg/kg oral dose of **16**, plasma concentrations exceeded the HWB IC_{80} of 24 nM for greater than 12 hours in the rat. With a 3 mg/kg oral dose in dog, plasma concentrations exceeded the IC_{80} for 24 hours (Figure 6). The prolonged exposure above levels corresponding to the HWB IC_{80} in both species were seen as an indicator that **16** was a viable molecule to test for efficacy in the clinic.

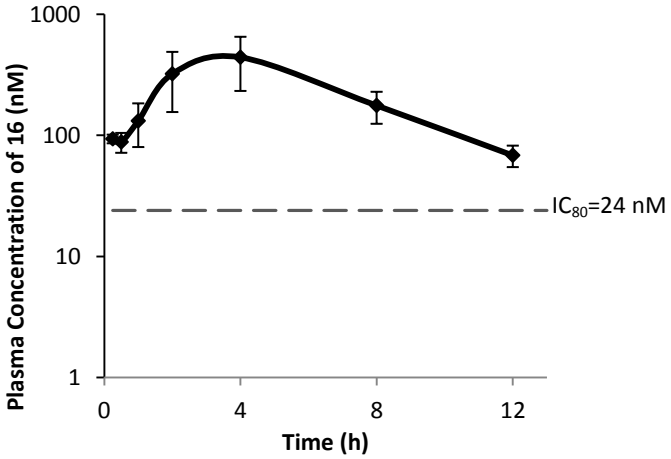

Figure 5. Plasma exposure of **16** in rat after a 5 mg/kg oral dose

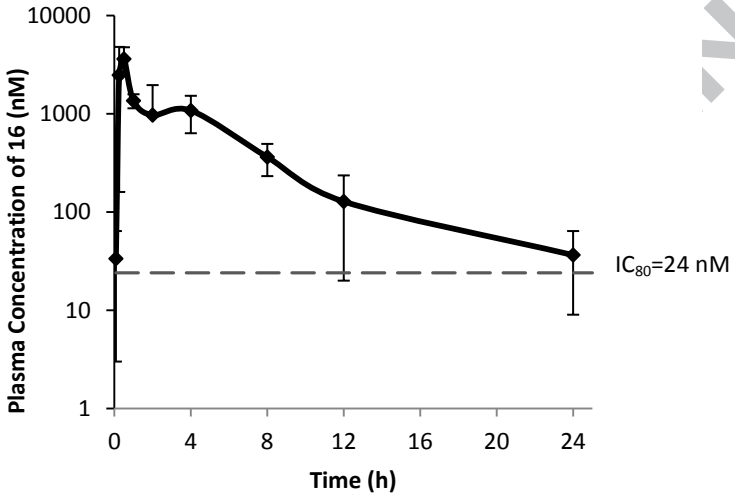

Figure 6. Plasma exposure of **16** in dog after a 3 mg/kg oral dose

Compound **16** was readily synthesized from accessible precursors (Scheme 1). Dess–Martin Periodinane-mediated oxidation of alcohol **17** generated aldehyde **18** in quantitative yield. Wittig reaction between **18** and the *in situ*-generated ylide derived from phosphonium salt **19** furnished intermediate **20** in 59 % yield as an inconsequential 5:1 mixture of the *E* and *Z* isomers. Hydrogenation of the olefin followed by removal of the Boc protecting group gave amine hydrochloride intermediate **21** in quantitative yield over two steps. Nucleophilic aromatic substitution of piperidine **22** with 2-chloro-8-methyl quinolone **23** and subsequent ester hydrolysis yielded carboxylic acid **25**. Finally, propylphosphonic anhydride-promoted coupling

between amine **21** and carboxylic acid **25** yielded intermediate **26** in 84% yield. Subsequent hydrolysis with sodium hydroxide afforded **16** in 96% yield and >99% purity.

Scheme 1. Synthesis of compound 16

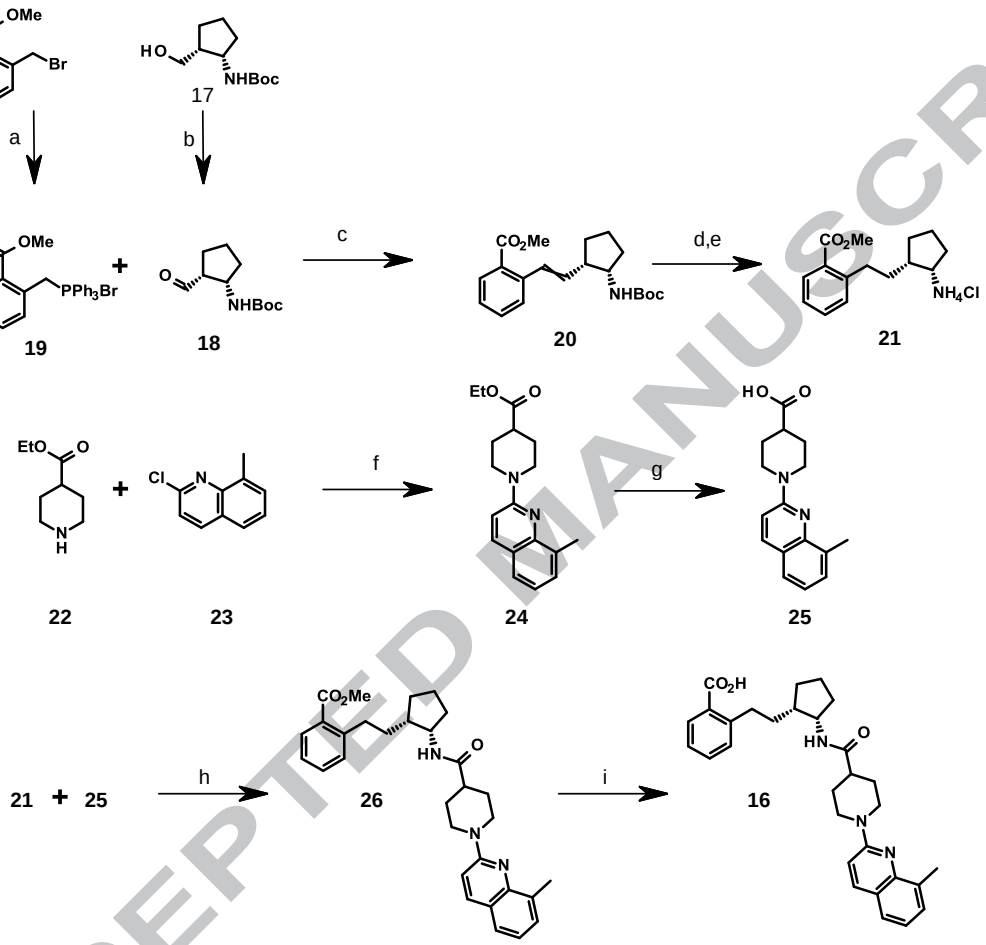

[a] PPh_3, Toluene, reflux, 76% yield [b] Dess-Martin Periodinane, CH_2Cl_2, –5 °C, 100% yield [c] KO*t*Bu, THF, 59% yield [d] Pt/C, H_2, 30 psig, EtOAc [e] 4.0 M HCl in Dioxane, CH_2Cl_2, 100% yield over 2 steps [f] K_2CO_3, DMSO, 130 °C, 96% yield [g] NaOH, H_2O, MeOH, THF, 94% yield [h] 50% propylphosphonic anhydride in EtOAc, DIPEA, CH_2Cl_2, 0 °C →r.t., 84% yield [i] NaOH, THF, MeOH, H_2O, 94% yield

In summary, we have described a novel class of acidic mPGES-1 inhibitors with nanomolar enzymatic and HWB potency. Rational design led initially to the identification of anthranilic acid **5**, a nanomolar inhibitor of mPGES-1 inhibitor with micromolar HWB potency. Structural modifications improved the HWB affinity, reduced rat clearance and reduced the CYP2C9 liability. Because it exemplified these desirable qualities, compound **16** was characterized further

and found to exhibit, among other parameters, sufficient exposure relative to its potency to render it suitable for clinical development.

Experimental Details

Atomic coordinates and structure factors for compound **4, 5,** and **16** with mPGES-1 are available from the RSCB Protein Data Bank with accession codes 5T37, 5T36 and 5TL9. Synthesis protocols, compound characterization, and assay protocols have been published.[19]

Acknowledgements

Use of the Advanced Photon Source, an Office of Science User Facility operated for the U.S. Department of Energy (DOE) Office of Science by Argonne National Laboratory, was supported by the U.S. DOE under Contract No. DE-AC02-06CH11357. The beamline staff, Stephen Wasserman, John W. Koss, and Laura Morisco are gratefully acknowledged.

References

1. Dancevic, C. M.; McCulloch, D. R., *Arthritis Res. Ther.* **2014,** *16*, 429.
2. Kean, W. F.; Buchanan, W. W., *Inflammopharmacology* **2005,** *13*, 343
3. Ricciotti, E.; FitzGerald, G. A., *Arterioscler. Thromb. Vasc. Biol.* **2011,** *31*, 986.
4. Prusakiewicz, J. J.; Duggan, K. C.; Rouzer, C. A.; Marnett, L. J., *Biochemistry* **2009,** *48*, 7353.
5. Seibert, K.; Masferrer, J. L., *Receptor* **1994,** *4*, 17.
6. Matsui, H.; Shimokawa, O.; Kaneko, T.; Nagano, Y.; Rai, K.; Hyodo, I., *J. Clin. Biochem. Nutr.* **2011,** *48*, 107.
7. (a) Chen, Y. F.; Jobanputra, P.; Barton, P.; Bryan, S.; Fry-Smith, A.; Harris, G.; Taylor, R. S., *Health Technol. Assess.* **2008,** *12*, 1; (b) Hawkey, C. J., *Lancet* **1999,** *353*, 307.
8. (a) Yu, Y.; Ricciotti, E.; Scalia, R.; Tang, S. Y.; Grant, G.; Yu, Z.; Landesberg, G.; Crichton, I.; Wu, W.; Pure, E.; Funk, C. D.; FitzGerald, G. A., *Sci. Transl. Med.* **2012,** *4*, 132; (b) Sun, S. X.; Lee, K. Y.; Bertram, C. T.; Goldstein, J. L., *Curr. Med. Res. Opin.* **2007,** *23*, 1859.
9. Chen, Y.; Liu, H.; Xu, S.; Wang, T.; Li, W., *Med. Chem. Comm.* **2015,** *6*, 2081.
10. Jakobsson, P. J.; Thoren, S.; Morgenstern, R.; Samuelsson, B., *Proc. Natl. Acad. Sc.i U S A* **1999,** *96*, 7220.
11. Murakami, M.; Naraba, H.; Tanioka, T.; Semmyo, N.; Nakatani, Y.; Kojima, F.; Ikeda, T.; Fueki, M.; Ueno, A.; Oh, S.; Kudo, I., *J. Biol. Chem.* **2000,** *275*, 32783.
12. Kamei, D.; Yamakawa, K.; Takegoshi, Y.; Mikami-Nakanishi, M.; Nakatani, Y.; Oh-Ishi, S.; Yasui, H.; Azuma, Y.; Hirasawa, N.; Ohuchi, K.; Kawaguchi, H.; Ishikawa, Y.; Ishii, T.; Uematsu, S.; Akira, S.; Murakami, M.; Kudo, I., *J. Biol. Chem* **2004,** *279*, 33684.
13. (a) Chang, H. H.; Meuillet, E. J., *Fut. Med. Chem.* **2011,** *3*, 1909; (b) Wang, J. L.; Limburg, D.; Graneto, M. J.; Springer, J.; Hamper, J. R.; Liao, S.; Pawlitz, J. L.; Kurumbail, R. G.; Maziasz, T.; Talley, J. J.; Kiefer, J. R.; Carter, J., *Bioorg. Med. Chem. Let.* **2010,** *20*, 7159; (c) Riendeau, D.; Aspiotis, R.; Ethier, D.; Gareau, Y.; Grimm, E. L.; Guay, J.; Guiral, S.; Juteau, H.; Mancini, J. A.; Methot, N.; Rubin, J.; Friesen, R. W., *Bioorg. Med. Chem. Lett.* **2005,** *15*, 3352;

(d) Arhancet, G. B.; Walker, D. P.; Metz, S.; Fobian, Y. M.; Heasley, S. E.; Carter, J. S.; Springer, J. R.; Jones, D. E.; Hayes, M. J.; Shaffer, A. F.; Jerome, G. M.; Baratta, M. T.; Zweifel, B.; Moore, W. M.; Masferrer, J. L.; Vazquez, M. L., *Bioorg. Med. Chem. Lett.***2013,** *23*, 1114; (e) Schiffler, M. A.; Antonysamy, S.; Bhattachar, S. N.; Campanale, K. M.; Chandrasekhar, S.; Condon, B.; Desai, P. V.; Fisher, M. J.; Groshong, C.; Harvey, A.; Hickey, M. J.; Hughes, N. E.; Jones, S. A.; Kim, E. J.; Kuklish, S. L.; Luz, J. G.; Norman, B. H.; Rathmell, R. E.; Rizzo, J. R.; Seng, T. W.; Thibodeaux, S. J.; Woods, T. A.; York, J. S.; Yu, X. P., *J. Med. Chem*. **2016,** *59*, 194.

14. Chandrasekhar, S.; Harvey, A. K.; Yu, X. P.; Chambers, M. G.; Oskins, J. L.; Lin, C.; Seng, T. W.; Thibodeaux, S. J.; Norman, B. H.; Hughes, N. E.; Schiffler, M. A.; Fisher, M. J., *J. Pharm. Exp. Ther*. **2016,** *356*, 635.

15. Huntjens, D. R.; Danhof, M.; Della Pasqua, O. E., *Rheumatology (Oxford)* **2005,** *44*, 846.

16. Durham, T. B.; Blanco, M. J., *Bioorg. Med. Chem. Lett* **2015,** *25*, 998.

17. (a) Sjogren, T.; Nord, J.; Ek, M.; Johansson, P.; Liu, G.; Geschwindner, S., *Proc. Natl. Acad. Sci U S A* **2013,** *110* (10), 3806; (b) Luz, J. G.; Antonysamy, S.; Kuklish, S. L.; Condon, B.; Lee, M. R.; Allison, D.; Yu, X. P.; Chandrasekhar, S.; Backer, R.; Zhang, A.; Russell, M.; Chang, S. S.; Harvey, A.; Sloan, A. V.; Fisher, M. J., *J. Med. Chem.* **2015,** *58*, 4727.

18: For another example of an 8-methyl quinoline containing ligand of mPGES-1 see Kuklish, S.L.; Antonysamy, S.; Bhattachar, S.N.; Chandrasekhar, S.; Fisher, M.J.; Fretland, A.J.; Gooding, K.; Harvey, A.; Hughes, N.E.; Luz, J.G.; Manninen, P.R.; McGee, J.E.; Navarro, A.; Norman, B.H.; Partridge, K.M.; Quimby, S.J.; Schiffler, M.A.; Sloan, A.V.; Warshawsky, A.M.; York, J.S.; Yu, X.-P.; *Bioorg. Med. Chem. Lett.* **2016**, *26*, 4824

19. Fisher, M.J.; Kuklish, S.L.; Partridge, K.M.; York, J. S. Patent Number WO 2016069374 A1, 2016

Graphical Abstract